



**Precise Control of Cyclodextrin-Based Pseudo-Polyrotaxane
Lamellar Structure via Axis Polymer Composition**

Journal:	<i>Soft Matter</i>
Manuscript ID	SM-ART-07-2020-001388.R1
Article Type:	Paper
Date Submitted by the Author:	24-Aug-2020
Complete List of Authors:	Uenuma, Shuntaro; The University of Tokyo, Advanced Materials Science; Maeda, Rina; The University of Tokyo, Advanced Materials Science Yokoyama, Hideaki; The University of Tokyo, Ito, Kohzo; The University of Tokyo, Graduate School of Frontier Sciences

ARTICLE

Precise Control of Cyclodextrin-Based Pseudo-Polyrotaxane Lamellar Structure via Axis Polymer Composition

Shuntaro Uenuma,* Rina Maeda, Hideaki Yokoyama, Kohzo Ito*

Received 00th January 20xx,
Accepted 00th January 20xx

DOI: 10.1039/x0xx00000x

A self-assembly of cyclodextrin (CD) with guest polymers has attracted much attention owing to its biocompatibility and accessibility. In this study, we investigate the composition effect of poly(ethylene oxide)_m-poly(propylene oxide)_n-poly(ethylene oxide)_m (EO_mPO_nEO_m) triblock copolymers on lamellar or plate structures formed by complexation with β-CD. EO₅PO₂₉EO₅, EO₁₄PO₂₉EO₁₄, and EO₇₅PO₂₉EO₇₅ show periodic lamellar morphology consisting of single-crystalline pseudo-polyrotaxane (PPR) nanosheets with a thickness equal to the central PO length. This is because β-CDs selectively cover the PO component and cause the microphase separation between β-CD and EO layers. The thickness of the EO layers increases linearly with increasing number of EO units, which suggests that the EO chains are constrained into virtual cylinders with the diameter of the β-CD. This means that we can precisely control the thickness of both the crystal (β-CD and PO) and the amorphous (EO) layers in the lamellar structure. In contrast, EO₂PO₂₉EO₂ forms a thin plate structure, where not only PO but also EO chains are covered with β-CD. Furthermore, the length of the central PO component is necessary to form the lamellar structure with the phase separation between the β-CD and EO layers. These findings provide a more fundamental understanding to enhance the variety and applicability of CD-based self-assembled materials.

Introduction

Supramolecular self-assembly is a bottom-up process producing higher ordered structures.^{1–4} The forces of self-assembly are based on noncovalent interactions such as hydrogen bonding, hydrophobic, electrostatic, host-guest, and π-π interactions, as well as crystallization. Compared to structures created by top-down processes, materials fabricated via supramolecular self-assembly have the capability to dynamically modify the higher order structures induced by the change in parameters such as temperature, pressure, and concentration of the solutions.^{5–8} The design of the higher order structure is based on the choice of the building blocks and is one of the featured advantages of supramolecular self-assembled materials. Since the nano- and micro-scale structures affect the physical properties of the materials, several attempts were made in the past few decades to control the higher order structures.^{9–12} Block copolymers form various types of periodic arrangements through microphase separation between immiscible components. Higher order structures can be controlled by designing the copolymer composition.^{13–15} Hydrogen bonds and π-π interactions are also promising elements to control shape and geometry of the resulting higher order structure owing to their directionality. Rosettes consisting of hydrogen-bonded cyclic hexamers can form one-dimensional supramolecular polymers.¹⁶ Stupp *et al.* reported unique structures such as

fibers, nanotubes¹⁷ and mash-rooms¹⁸ strategically utilizing the hydrogen bonds incorporated in the building blocks.

Recently, crystallization-driven self-assembly has attracted much attention to construct two-dimensional (2D) materials that are to date difficult to produce via self-assembly.^{19–21} This concept is derived from the formation of the lamellar sheets of crystalline polymer that was reported over 60 years ago.²² By introducing crystalline segments into block copolymers they crystallize, and the other non-crystalline part disturbs the crystal growth of the whole chain, leading to the formation of a well-defined and distinct higher order structure, reflecting the single crystal structure.²³

Complexation of cyclodextrin (CD), a representative of a host molecule, with a guest polymer creates a self-assembled structure.^{24–28} The CD crystallizes based on the multi-point hydrogen bonds and forms a well-defined structure. Recently, our group reported that the complexation of CDs and polymers is a feasible way to control the morphology of the self-assembled structure.^{29–31} Especially, the selective inclusion of β-CD into the central propylene oxide (PO) segment of carboxyl-terminated poly(ethylene oxide)₇₅-block-poly(propylene oxide)₂₉-block-poly(ethylene oxide)₇₅ (COOH-EO₇₅PO₂₉EO₇₅; subscripts denote the number of monomer units) leads to the formation of nanosheet materials, which are called pseudo-polyrotaxane (PPR) nanosheets, because of the stronger interaction of β-CD with PO than with EO.³⁰ The thickness and rhombus-like shape of the nanosheet are determined by the length of the PO segment and the single crystal structure of the β-CD, respectively.

Although the selective inclusion of β-CDs into the triblock copolymer generated the nanosheet structure, the EO and PO

Department of Advanced Materials Science, Graduate School of Frontier Sciences, The University of Tokyo, Kashiwa-city, Chiba 277-8561, Japan. E-mail: s-uenuma@g.ecc.u-tokyo.ac.jp, kohzo@k.u-tokyo.ac.jp; Tel: +81-4-7136-3757

chain length effect of the EOPEO triblock copolymer was not examined. To control the morphology, geometry, and d -space of the CD-based self-assembled structure, it is necessary to understand the axis effects of the triblock copolymer composition in the higher order structure. In this study, we investigated how the EO and PO segment length of EOPEO affects the higher order structure formed by the complexation with β -CD. $\text{EO}_m\text{PO}_{29}\text{EO}_m$ with a variety of m units was used to systematically study the effect of the EO segment length. Furthermore, since $\text{EO}_{11}\text{PO}_{16}\text{EO}_{11}$ and $\text{EO}_5\text{PO}_{29}\text{EO}_5$ have the same chain length but a different composition, the structures of their β -CD complex were compared to assess the effect of PO chain length on the self-assembly. The samples were prepared by just mixing the axis copolymers and β -CD in water. The crystal and meso-scale structures of the aqueous samples were analyzed using wide and small angle X-ray scattering (WAXS and SAXS). The micro-order morphologies were observed using scanning electron microscopy (SEM).

Results and discussion

EO chain length effect of $\text{EO}_m\text{PO}_{29}\text{EO}_m$

To systematically investigate the effect of EO chain length, a series of $\text{EO}_m\text{PO}_{29}\text{EO}_m$ triblock copolymers with the same PO length ($\text{EO}_2\text{PO}_{29}\text{EO}_2$, $\text{EO}_5\text{PO}_{29}\text{EO}_5$, $\text{EO}_{14}\text{PO}_{29}\text{EO}_{14}$, and $\text{EO}_{20}\text{PO}_{29}\text{EO}_{20}$) was used and the structures of their complexes with β -CD were analyzed. The samples were named $\beta\text{CD}/\text{EO}_2\text{PO}_{29}\text{EO}_2$, $\beta\text{CD}/\text{EO}_5\text{PO}_{29}\text{EO}_5$, $\beta\text{CD}/\text{EO}_{14}\text{PO}_{29}\text{EO}_{14}$, and $\beta\text{CD}/\text{EO}_{20}\text{PO}_{29}\text{EO}_{20}$, respectively.

The crystal structures of the aqueous samples were analyzed using WAXS (Figure 1). All samples show the characteristic peaks (the crystal planes are indicated in Figure 1, where parenthesis denote the crystal planes that have relatively weak intensities) derived from the conventional crystal structure of β -CD with polymers (monoclinic, $a = 1.910$ nm, $b = 2.426$ nm, $c = 1.568$ nm, $\alpha = \gamma = 90^\circ$, $\beta = 111^\circ$).³² As shown in Figure 1, the 001 peak ($2\theta = 5.9^\circ$), whose reciprocal vector is parallel to the β -CDs' height direction, becomes broader as the EO chain length increases, especially for $\beta\text{CD}/\text{EO}_{20}\text{PO}_{29}\text{EO}_{20}$. This means that the crystallite size in the direction perpendicular to the 001 plane decreases.

The morphologies of the dried samples were observed using SEM (Figure 2). $\beta\text{CD}/\text{EO}_2\text{PO}_{29}\text{EO}_2$ and $\beta\text{CD}/\text{EO}_5\text{PO}_{29}\text{EO}_5$ form plate structures with an edge length from 1 to 2 μm and display a rhombus shape. The shape reflects the single crystal structure of the β -CD shown in the WAXS experiments.^{32,33} In the cases of $\beta\text{CD}/\text{EO}_{14}\text{PO}_{29}\text{EO}_{14}$ and $\beta\text{CD}/\text{EO}_{20}\text{PO}_{29}\text{EO}_{20}$, thinner plate or sheet structures with similar shape are observed. This correlates with the broader 001 peak of $\beta\text{CD}/\text{EO}_{20}\text{PO}_{29}\text{EO}_{20}$ compared to that of $\beta\text{CD}/\text{EO}_2\text{PO}_{29}\text{EO}_2$ (Figure 1). The SEM observations confirm the formation of the ordered microstructures based on the single crystal structure of β -CD.

Next, to analyze the mesoscale structure, SAXS experiments were performed with the aqueous samples (Figure 3). The SAXS profile of $\beta\text{CD}/\text{EO}_2\text{PO}_{29}\text{EO}_2$ shows no peaks and fringes, which means that there are no periodic phase-separated structures. In

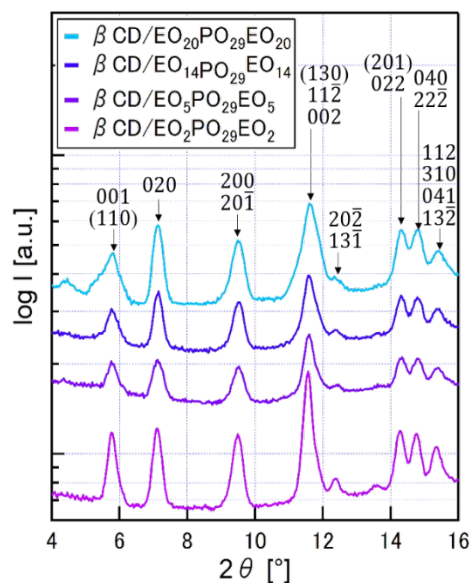


Figure 1. WAXS profiles of $\beta\text{CD}/\text{EO}_2\text{PO}_{29}\text{EO}_2$, $\beta\text{CD}/\text{EO}_5\text{PO}_{29}\text{EO}_5$, $\beta\text{CD}/\text{EO}_{14}\text{PO}_{29}\text{EO}_{14}$, and $\beta\text{CD}/\text{EO}_{20}\text{PO}_{29}\text{EO}_{20}$.

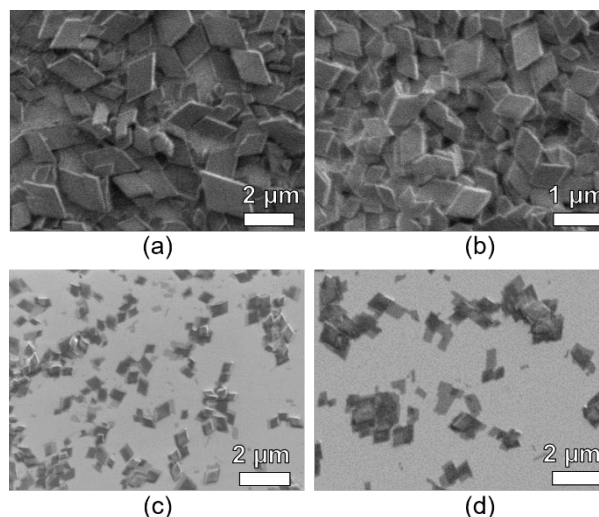


Figure 2. SEM images of (a) $\beta\text{CD}/\text{EO}_2\text{PO}_{29}\text{EO}_2$, (b) $\beta\text{CD}/\text{EO}_5\text{PO}_{29}\text{EO}_5$, (c) $\beta\text{CD}/\text{EO}_{14}\text{PO}_{29}\text{EO}_{14}$, and (d) $\beta\text{CD}/\text{EO}_{20}\text{PO}_{29}\text{EO}_{20}$.

contrast, other samples exhibit the structure and form factors of regular structures. It is generally known that β -CD covers PO chains but not those of EO.³⁴ Therefore, if β -CD covers only the PO chains of $\text{EO}_m\text{PO}_{29}\text{EO}_m$, single-crystalline PPR nanosheets of a thickness equal to the PO chain length should be formed because of the microphase separation between β -CD and EO chains.³⁰ Moreover, when the PPR nanosheets are stacked, the lamellar structure consisting of both the crystal (β -CD and PO) and EO layers should be yielded.³⁰ However, $\beta\text{CD}/\text{EO}_2\text{PO}_{29}\text{EO}_2$ does not generate such lamellar structures, although it shows the plate structure in SEM. This suggests that β -CDs possibly covered the whole axis chain including 2 EO units (Figure 4a). It was reported that β -CD covers EO chains at specific conditions.³⁵ In this case, the plate crystal of β -CD without phase separation was possibly formed, gaining a large

crystallization enthalpy which balanced the disadvantage that β -CDs covered unfavorable EO segments.

The SAXS profiles of β CD/EO₅PO₂₉EO₅ and β CD/EO₁₄PO₂₉EO₁₄, on the other hand, display primary peaks at $q^* = 0.050 \text{ \AA}^{-1}$ and 0.043 \AA^{-1} and their secondary peaks are observed at twice the q values of the primary ones. This indicated that lamellar structures with a d -spacing of 12.6 nm and 14.5 nm were formed with respect to β CD/EO₅PO₂₉EO₅ and β CD/EO₁₄PO₂₉EO₁₄, generating nanosheet structures with stacking (Figure 4b). The β -CDs should selectively cover the central 29 PO units and not EO chains with more than or equal to 5 units. β CD/EO₂₀PO₂₉EO₂₀ exhibit the broad primary peak at $q = 0.032 \text{ \AA}^{-1}$ (corresponding to the d -spacing of 19.6 nm, indicated as arrow in Figure 3a). Further, the fringe is observed and well fitted by the calculated sheet form factor³⁶ with the thickness of 10.4 nm (Figure 3b). This indicated that a PPR nanosheet with a thickness approximately corresponding to that of the stretched length of PO₂₉ (11 nm) was formed.

The d -spacing of the lamellar structures formed in the sample becomes longer as the EO chain length increases. As we reported in our previous paper³⁰, the complex between β -CD and OH-EO₇₅PO₂₉EO₇₅ (β CD/EO₇₅PO₂₉EO₇₅) yields a lamellar structure with a d -spacing of 40 nm. Figure 5a indicates the plots of the d -spacing of the lamellar structures vs the twice m values, the latter meaning the monomer units in the EO layer. A linear relationship was observed with a vertical intercept of 10.4 nm and a slope of 0.198 nm. The vertical intercept is consistent with the β -CD layer thickness that equals the PO chain length, and the slope means the increase in the EO layer thickness per EO monomer. According to the scaling theory of the blob model of the polymer brush, the number of chain monomers and the chain height display a linear relationship.^{37,38} Since the average distance, 1.5 nm, between β -CDs in the PPR nanosheet is shorter than the average size of EO chains in the dilute solution, even for EO₅PO₂₉EO₅, it is reasonable to consider that the EO chains are constrained in the virtual cylinder with the diameter of the β -CD and their heights can be theoretically described by the blob theory of the polymer brush (Figure 5b). To the best of our knowledge, this is the first study of the polymer brush to immobilize the chain ends to the surface at the periodic position, which corresponds to the aligned cavities of the β -CD columnar crystal and to have the brush density dependent only on the β -CD crystal structure irrespective of EO chain length.

In the case of the dried state EO on the β -CD layer, the height increase per EO unit was calculated to be 0.031 nm using the weight density (1.2 g/cm^3)³⁹ and brush density of EO chains. The ratio of the EO layer thickness per EO unit in the dried state to that in water is 14.2%. This is the volume fraction of EO chains in the EO layer in water, which means that 85.8% of water is included in the EO layer. Furthermore, the linear relationship in water in Figure 5a indicates that the swelling ratio is constant, regardless of the EO chain length with $5 \leq m \leq 75$. The driving force to form the lamellar structure is considered to be based on the large van der Waals force between EO layers, which is generally observed for inorganic nanosheet particles.⁴⁰

Using the series of the EO _{m} PO₂₉EO _{m} triblock copolymer, we revealed the effect of EO chain length on the lamellar structure

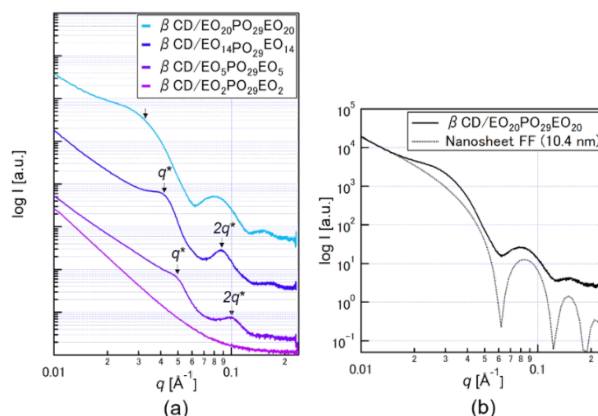


Figure 3. (a) SAXS profiles of β CD/EO₂₀PO₂₉EO₂₀, β CD/EO₅PO₂₉EO₅, β CD/EO₁₄PO₂₉EO₁₄, and β CD/EO₂₀PO₂₉EO₂₀. (b) Fitting result of nanosheet form factor to the experimental profile of β CD/EO₂₀PO₂₉EO₂₀.

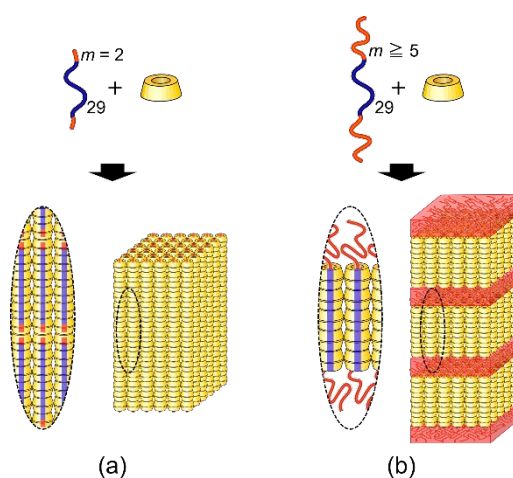


Figure 4. Schematic illustrations of (a) plate structures formed in β CD/EO₂PO₂₉EO₂ and (b) nanosheet structures formed in β CD/EO₅PO₂₉EO₅, β CD/EO₁₄PO₂₉EO₁₄, β CD/EO₂₀PO₂₉EO₂₀, and β CD/EO₇₅PO₂₉EO₇₅.

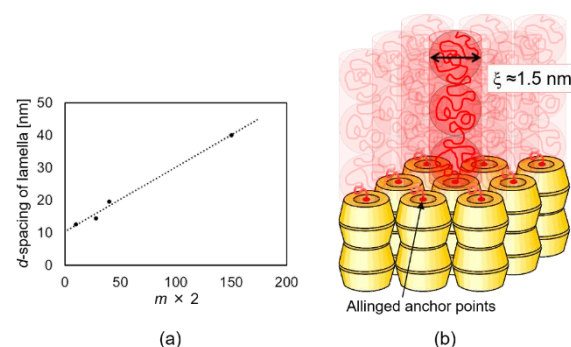


Figure 5. (a) Plots of the d -spacing of the lamellar structure of the β -CD/EO _{m} PO₂₉EO _{m} series. (b) Schematic illustration of the blob model that describes the configuration of the EO chains on the β -CD columnar crystals.

of the complex with β -CD. The short EO chains of EO₂PO₂₉EO₂ were covered with β -CDs to gain a large enthalpy resulting in the formation of the plate crystal without the phase-separated lamellar structures. On the other hand, EO _{m} PO _{n} EO _{m} with $m > 5$ (EO₅PO₂₉EO₅, EO₁₄PO₂₉EO₁₄, EO₂₀PO₂₉EO₂₀, and EO₇₅PO₂₉EO₇₅) led to the formation of microphase separated structures with lamellar morphology including the formation of the β -CD nanosheets. We recently reported that the axis polymer with

the end group of the low binding constant to β -CD formed the nanosheet structure without stacking.²⁹ In this study, we revealed that the longer end chains that have a low binding constant are more favourable than the short ones for forming the β -CD nanosheets.

In this study, it was confirmed that the thickness of EO layers of the lamellar structure can be precisely controlled by changing the length of EO segments in the triblock copolymer. The height of swollen EO brush is well described by the blob model of the polymer brush. This is because EO chains were tethered at the periodic positions corresponding to the aligned cavity of the β -CD columnar crystal. While, the β -CD nanosheet thickness is determined by the stretched length of the central PO chain. The results of this study suggest that each layer thickness of this lamellar structure can be precisely and independently tuned by designing the axis polymer compositions.

Effect of the PO chain length of $EO_mPO_nEO_m$

To investigate the effect of the PO chain length of the EOPEO triblock copolymer on the self-assembled structure, we compared $EO_{11}PO_{16}EO_{11}$ and $EO_5PO_{29}EO_5$. The complex between β -CD and $EO_{11}PO_{16}EO_{11}$ was prepared (β CD/ $EO_{11}PO_{16}EO_{11}$) to analyze the structure.

The formation of the conventional monoclinic crystal structure of β -CDs was confirmed using WAXS (Figure 6a). However, the SAXS profile of β CD/ $EO_{11}PO_{16}EO_{11}$ does not have any peaks and form factor (Figure 6b) and the SEM image shows plate crystals (Figure 6c). These results suggested that β -CDs in β CD/ $EO_{11}PO_{16}EO_{11}$ cover not only PO segments but also EO ones similar to β CD/ $EO_2PO_{29}EO_2$, although β CD/ $EO_{11}PO_{16}EO_{11}$ has longer EO chains than β CD/ $EO_2PO_{29}EO_2$.

If β -CDs selectively cover the short (16 units) PO chain of $EO_{11}PO_{16}EO_{11}$ and not EO chains, the thickness of the resulting

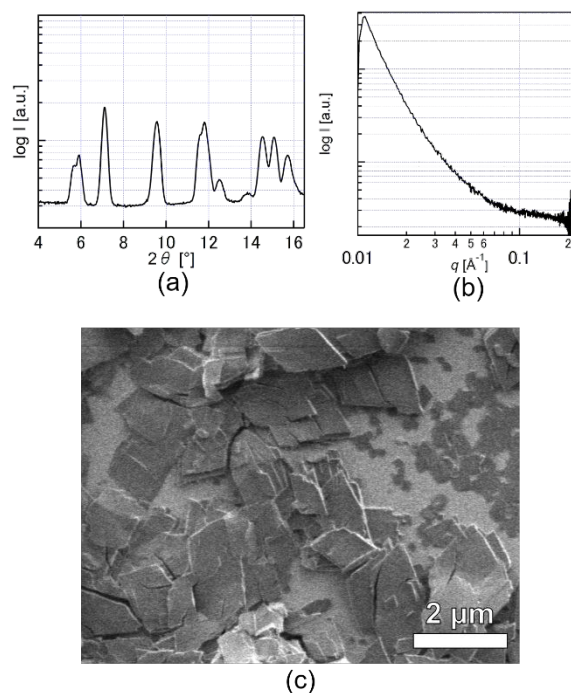


Figure 6. (a) WAXS profile, (b) SAXS profile and (c) SEM image of β CD/ $EO_{11}PO_{16}EO_{11}$.

nanosheet should be quite thin (5.6 nm, Figure 7a). Such a thin nanosheet is unstable because the sum of the enthalpy gain of crystallization and host-guest interaction between β -CD and PO chain should not exceed the surface energy of the nanosheet. Instead, the plate crystals without a microphase separation are formed by covering EO chains with β -CD. The plate crystals without meso-scale phase separation can achieve both a large enthalpy gain and surface energy reduction (Figure 7b).

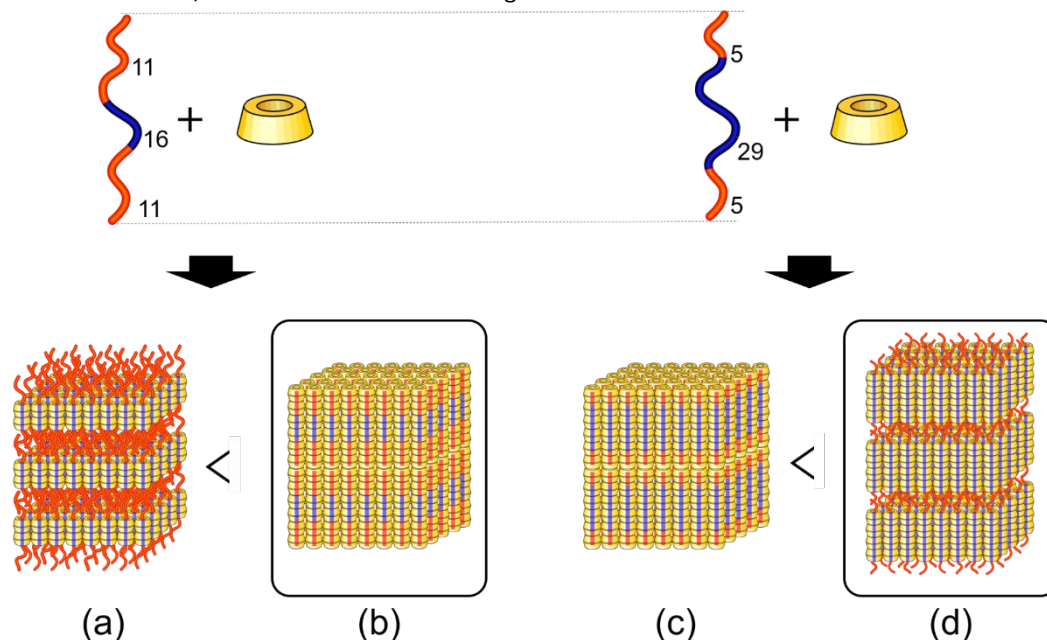


Figure 7. Schematic illustrations of the structures of β CD/ $EO_{11}PO_{16}EO_{11}$ and β CD/ $EO_5PO_{29}EO_5$. If β -CD covers only the PPO segment of the $EO_{11}PO_{16}EO_{11}$, structure (a) should be formed. However, structure (b) is formed in the case of β -CD/ $EO_{11}PO_{16}EO_{11}$ even though the β -CD covers the unfavourable EO segment. For β CD/ $EO_5PO_{29}EO_5$, (c) was not formed where the β -CD fully covers the whole axis including the PEO segment. In the case of β CD/ $EO_5PO_{29}EO_5$, (d) is more stable where β -CD covers only the PPO segment and the phase separated structures are formed.

Next, the structures of β CD/EO₁₁PO₁₆EO₁₁ and β CD/EO₅PO₂₉EO₅ were compared. If the whole EO₅PO₂₉EO₅ chain is covered with β -CDs (Figure 7c), the structure of EO₅PO₂₉EO₅ should be more stable than that of β CD/EO₁₁PO₁₆EO₁₁, as illustrated in Figure 7b, owing to the stronger host-guest interaction between β -CD and PO compared to that between β -CD and EO. However, β -CDs of β CD/EO₅PO₂₉EO₅ formed the microphase separated structure with the lamellar morphology (Figure 7d), which indicates that β -CDs of β CD/EO₅PO₂₉EO₅ do not cover the EO segments. This suggests that phase separation occurs when the PO length is long enough to obtain the host-guest enthalpy through complexation between β -CD and PO segments in order to overcome the surface energy. The length of the central PO also significantly affects the resulting morphologies of the complex of β -CD with EO_{*m*}PO_{*n*}EO_{*m*}.

Effect of the PO homopolymer chain length

To investigate the self-assembled structure consisting of homopolymers, complexes between β -CD and PO homopolymers with different lengths (β CD/PO₇, β CD/PO₁₃, β CD/PO₃₄, and β CD/PO₆₉, the numbers denote the number of monomer units) were prepared to analyze their structures. The WAXS profiles of all samples show the characteristic peaks of a monoclinic crystal (Figure 8). Therefore, it was confirmed that the complex between β -CD and the PO homopolymer formed the monoclinic crystal structure irrespective of the PO chain length.

In the SEM images of β CD/PO₇, β CD/PO₁₃, and β CD/PO₃₄, micro-ordered sheet structures with well-defined shapes were observed (Figure 9a-c). In contrast, when the number of monomer units of the PO exceeds 69, SEM images show disordered structures (Figure 9d). It is known that when the axis polymer is hydrophobic and long, the competition between the crystal growth of CD and the hydrophobic aggregation of the axis polymer causes the formation of polycrystalline structures.³¹ Hence, the present results indicated that a PO homopolymer shorter than 34 units is necessary to form a well-defined micro-ordered structure. However, the SAXS profiles of all samples showed no peaks and fringes (Figure 10). This indicates the absence of microphase-separated structures and inconsistent plate thicknesses. To form a nanosheet structure with uniform thickness, EO segments must be attached to the PO polymer.

Conclusions

We investigated the effect of EO and PO chain length of EO_{*m*}PO_{*n*}EO_{*m*} triblock copolymers on the higher order structure formed by the complexation with β -CD. To form lamellar structures, the EO chains of EO_{*m*}PO₂₉EO_{*m*} should exceed a certain length. When $m > 5$, lamellar structures consisting of crystalline β -CD pseudo-polyrotaxane nanosheets and amorphous EO layers were formed. The thickness of the EO layer linearly increased with the increase in EO chain unit number. This was due to the fact that the EO chains were constrained in the virtual cylinder with the diameter of the β -

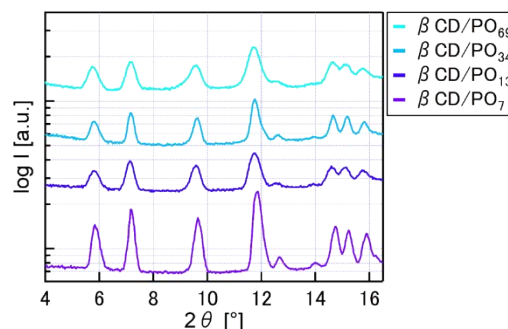


Figure 8. WAXS profiles of β CD/PO₇, β CD/PO₁₃, β CD/PO₃₄, and β CD/PO₆₉.

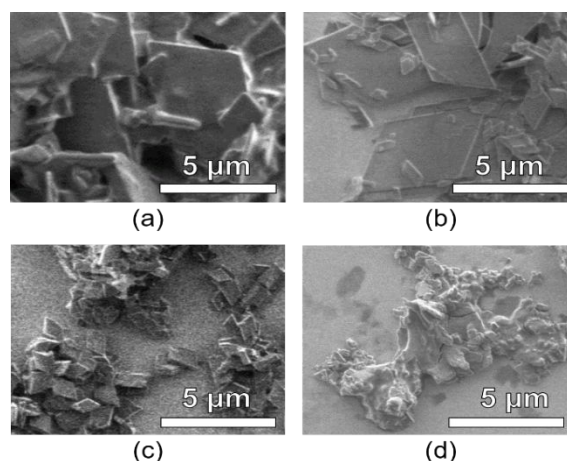


Figure 9. SEM images of β CD/PO₇, β CD/PO₁₃, β CD/PO₃₄, and β CD/PO₆₉.

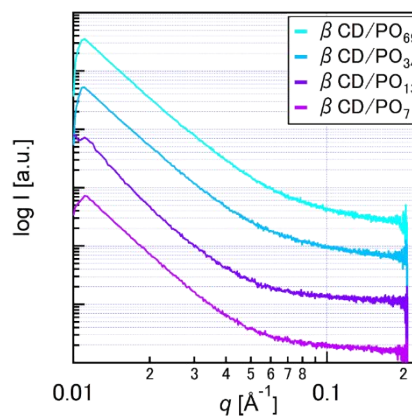


Figure 10. SAXS profiles of β CD/PO₇, β CD/PO₁₃, β CD/PO₃₄, and β CD/PO₆₉.

CD. The linear relationship between the thickness and the number of chain units followed the blob model of the polymer brush. Meanwhile, the β -CD nanosheet thickness was determined by the extended length of the central PO chain. These facts indicated that the thicknesses of each layer could be precisely and independently controlled. This was achieved due to the selective inclusion of β -CD to the PO segment and the periodically anchored polymer brush templated by the β -CD columnar crystal. Using the PO homopolymer, it was confirmed that homopolymers do not show microphase separation and

formation of nanosheets. These findings will aid the applied research on CD-based self-assembled materials and devices such as polymer composites, chemical sensors, drug delivery systems, and biomaterials.

MATERIALS AND METHODS

Materials

β -CD was purchased from Fujifilm Wako Pure Chemical Corporation. $\text{EO}_2\text{PO}_{29}\text{EO}_2$, $\text{EO}_5\text{PO}_{29}\text{EO}_5$, $\text{EO}_{14}\text{PO}_{29}\text{EO}_{14}$, $\text{EO}_{20}\text{PO}_{29}\text{EO}_{20}$, PO_7 , PO_{13} , PO_{34} , and PO_{69} were purchased from Sigma-Aldrich. The polydispersity indices of PO_{34} and PO_{69} were 1.1 and 1.2, respectively. All reagents were used as received.

Preparation of PPR

$\beta\text{CD}/\text{EO}_2\text{PO}_{29}\text{EO}_2$, $\beta\text{CD}/\text{EO}_5\text{PO}_{29}\text{EO}_5$, $\beta\text{CD}/\text{EO}_{14}\text{PO}_{29}\text{EO}_{14}$, and $\beta\text{CD}/\text{EO}_{20}\text{PO}_{29}\text{EO}_{20}$ were prepared by the following procedure: βCD was dissolved in deionized water (pH was approximately 7) at 23 ± 1 °C. The β -CD concentration was 8.8 mg mL^{-1} . An amount of 1 mg of $\text{EO}_2\text{PO}_{29}\text{EO}_2$, $\text{EO}_5\text{PO}_{29}\text{EO}_5$, $\text{EO}_{14}\text{PO}_{29}\text{EO}_{14}$, and $\text{EO}_{20}\text{PO}_{29}\text{EO}_{20}$ was added to 1 mL of aqueous β -CD, respectively. The mixed solutions were vigorously shaken by a vortex for 1 min. Further, the solutions were placed on a shaker and aged for 1 month. $\beta\text{CD}/\text{PO}_7$, $\beta\text{CD}/\text{PO}_{13}$, $\beta\text{CD}/\text{PO}_{34}$, and $\beta\text{CD}/\text{PO}_{69}$ were prepared by the following procedure: βCD was dissolved in deionized water (pH was approximately 7) at 23 ± 1 °C. The β -CD concentration was 18 mg mL^{-1} . An amount of 1 mg of $\text{EO}_{11}\text{PO}_{16}\text{EO}_{11}$, PO_7 , PO_{13} , PO_{34} , and PO_{69} was added to 1 mL of aqueous β -CD, respectively. The mixed solutions were vigorously shaken by a vortex for 1 min. Then, the solutions were deposited on a shaker and aged for 1 month. In all cases the solution became turbid after aging.

Sample preparation for structural analysis

The samples for the SEM experiments were prepared by dipping a silicone oxide substrate into an aqueous PPR dispersion. For X-ray experiments, the samples were concentrated by centrifuge to achieve enough intensity for analysis. The sample concentrations after centrifugation were obtained measuring the weight of the sample dried from 200 μL of an aqueous dispersion of PPRs. Then, the sample concentrations were adjusted to 10 wt% by adding deionized water. The 10 wt% aqueous PPR dispersions were transferred into a glass capillary for X-ray measurements (WJM-Glass Müller GmbH borosilicate capillary: $\varphi = 2.0 \times \text{length} = 80 \text{ mm}$) and used for SAXS and WAXS analysis.

Measurement

WAXS and SAXS experiments were carried out using a Rigaku NANOPIX instrument with a Hypix-3000 detector. The sample-to-detector distance was calibrated relative to the silver behenate peak. SEM observation was conducted with a JEOL JSM-7800F instrument.

Conflicts of interest

There are no conflicts of interest to declare.

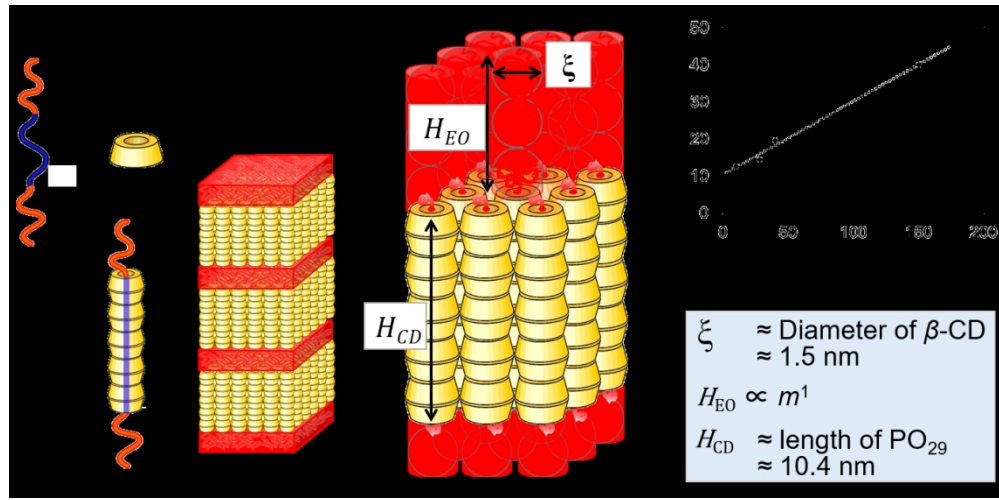
Acknowledgements

This work was supported by JST-Mirai Program Grant Number JPMJMI18A2, JSPS KAKENHI Grant Numbers JP19H00907, JP19K15618 and JP19J12840, and by OPERANDO-OIL.

Notes and references

- R. Chakrabarty, P. S. Mukherjee and P. J. Stang, *Chem. Rev.*, 2011, **111**, 6810–6918.
- A. J. Blake, N. R. Champness, P. Hubberstey, W. S. Li, M. A. Withersby and M. Schröder, *Coord. Chem. Rev.*, 1999, **183**, 117–138.
- V. Luzzati, *J. Cell Biol.*, 1962, **12**, 207–219.
- R. P. Rand and V. A. Parsegian, *Biochim. Biophys. Acta - Rev. Biomembr.*, 1989, **988**, 351–376.
- K. Kataoka, A. Harada and Y. Nagasaki, *Adv. Drug Deliv. Rev.*, 2012, **64**, 37–48.
- T. Fukui, S. Kawai, S. Fujinuma, Y. Matsushita, T. Yasuda, T. Sakurai, S. Seki, M. Takeuchi and K. Sugiyasu, *Nat. Chem.*, 2017, **9**, 493–499.
- G. Yu, K. Jie and F. Huang, *Chem. Rev.*, 2015, **115**, 7240–7303.
- Y. Wei, J. Tian, Z. Zhang, C. Zhu, J. Sun and Z. Li, *Macromolecules*, 2019, **52**, 1546–1556.
- S. Srivastava and N. A. Kotov, *Soft Matter*, 2009, **5**, 1146.
- M. A. Boles, M. Engel and D. V. Talapin, *Chem. Rev.*, 2016, **116**, 11220–11289.
- T. Kato, N. Mizoshita and K. Kishimoto, *Angew. Chemie Int. Ed.*, 2006, **45**, 38–68.
- Y. Orimo and A. Hotta, *Macromolecules*, 2011, **44**, 5310–5317.
- L. Leibler, *Macromolecules*, 1980, **13**, 1602–1617.
- F. Bates, *Annu. Rev. Phys. Chem.*, 1990, **41**, 525–557.
- A. K. Khandpur, S. Foerster, F. S. Bates, I. W. Hamley, A. J. Ryan, W. Bras, K. Almdal and K. Mortensen, *Macromolecules*, 1995, **28**, 8796–8806.
- S. Yagai, Y. Kitamoto, S. Datta and B. Adhikari, *Acc. Chem. Res.*, 2019, **52**, 1325.
- S. Ganda, M. Dulle, M. Drechsler, B. Förster, S. Förster and M. H. Stenzel, *Macromolecules*, 2017, **50**, 8544–8553.
- S. I. Stupp, *Science*, 1997, **276**, 384–389.
- Z. M. Hudson, C. E. Boott, M. E. Robinson, P. A. Rupar, M. A. Winnik and I. Manners, *Nat. Chem.*, 2014, **6**, 893–898.
- X. He, M. S. Hsiao, C. E. Boott, R. L. Harniman, A. Nazemi, X. Li, M. A. Winnik and I. Manners, *Nat. Mater.*, 2017, **16**, 481–488.
- T. Zhou, H. Qi, L. Han, D. Barbash and C. Y. Li, *Nat. Commun.*, 2016, **7**, 1–8.
- D. J. Blundell, A. Keller and A. J. Kovacs, *Polym. Lett.*, 1966, **4**, 481–486.
- G. Guerin, P. A. Rupar, I. Manners and M. A. Winnik, *Nat. Commun.*, 2018, **9**, 1158.
- A. Harada and M. Kamachi, *Macromolecules*, 1990, **23**, 2821–2823.
- S. Takahashi, N. L. Yamada, K. Ito and H. Yokoyama, *Macromolecules*, 2016, **49**, 6947–6952.

- 26 M. Oster, A. Hébraud, S. Gallet, A. Lapp, E. Pollet, L. Avérous and G. Schlatter, *Macromol. Rapid Commun.*, 2015, **36**, 292–297.
- 27 S. Yang, Y. Yan, J. Huang, A. V. Petukhov, L. M. J. Kroon-Batenburg, M. Drechsler, C. Zhou, M. Tu, S. Granick and L. Jiang, *Nat. Commun.*, 2017, **8**, 15856.
- 28 J. Wang and X. Zhang, *ACS Nano*, 2015, **9**, 11389–11397.
- 29 S. Uenuma, R. Maeda, H. Yokoyama and K. Ito, *Macromolecules*, 2019, **52**, 3881–3887.
- 30 S. Uenuma, R. Maeda, H. Yokoyama and K. Ito, *Chem. Commun.*, 2019, **55**, 4158–4161.
- 31 S. Uenuma, R. Maeda, H. Yokoyama and K. Ito, *Polymer*, 2019, **179**, 121689.
- 32 C.-C. Tsai, S. Leng, K.-U. Jeong, R. M. Van Horn, C.-L. Wang, W.-B. Zhang, M. J. Graham, J. Huang, R.-M. Ho, Y. Chen, B. Lotz and S. Z. D. Cheng, *Macromolecules*, 2010, **43**, 9454–9461.
- 33 M. Ohmura, Y. Kawahara, K. Okude, Y. Hasegawa, M. Hayashida, R. Kurimoto and A. Kawaguchi, *Polymer*, 2004, **45**, 6967–6975.
- 34 A. Harada, M. Okada, J. Li and M. Kamachi, *Macromolecules*, 1995, **28**, 8406–8411.
- 35 K. A. Udachin, L. D. Wilson and J. A. Ripmeester, *J. Am. Chem. Soc.*, 2000, **122**, 12375–12376.
- 36 N. Miyamoto and T. Nakato, *Isr. J. Chem.*, 2012, **52**, 881–894.
- 37 M. Daoud and P. G. De Gennes, *J. Phys.*, 1977, **38**, 85–93.
- 38 S. Patel, M. Tirrell and G. Hadziioannou, *Colloids and Surfaces*, 1988, **31**, 157–179.
- 39 H. Tadokoro, Y. Chatani, T. Yoshihara, S. Tahara and S. Murahashi, *Makromol. Chem.*, 1964, **73**, 109.
- 40 P. H. Nadeau, M. J. Wilson, W. J. McHardy and J. M. Tait, *Science*, 1984, **225**, 923–925.



238x117mm (150 x 150 DPI)